

A dual-band modified-rectangular patch with parasitic antenna for 2.4/5 GHz wireless local area network applications

Suthasinee Lamultree¹, Sakolkorn Ungprasutr¹, Charinsak Saetiaw¹, Chuwong Phongcharoenpanich²

¹Department of Electronics and Telecommunication Engineering, Faculty of Engineering, Rajamangala University of Technology Isan Khonkaen Campus, Khonkaen, Thailand

²Department of Telecommunications Engineering, School of Engineering, King Mongkut's Institute of Technology Ladkrabang, Bangkok, Thailand

Article Info

Article history:

Received Mar 5, 2025

Revised Aug 31, 2025

Accepted Sep 10, 2025

Keywords:

2.4/5 WLAN

Dual-band antenna

Modified-rectangular patch

Omnidirectional antenna

Parasitic element

Patch antenna

ABSTRACT

This research presents the design and implementation of a dual-band patch antenna (DBPA) optimized for 2.4 GHz and 5 GHz wireless local area network (WLAN) applications. The antenna features a modified rectangular patch with a cut corner and two parasitic rectangular patches, enabling dual-band operation with enhanced gain. The DBPA is fed by a 50-Ohm coplanar waveguide and fabricated on a single-layer copper circuit board using a flame-retardant 4 substrate with a relative permittivity of 4.3 and a thickness of 1.6 mm. A prototype with compact dimensions of $0.040 \times 0.040 \times 0.0009 \lambda^3$ was constructed and experimentally evaluated. Measurements reveal a nearly omnidirectional radiation pattern, achieving peak gains of 2.92 dBi at 2.4 GHz and 4.25 dBi at 5 GHz. The antenna demonstrates a wide 10 dB return loss bandwidth of 67.7% (1.7–3.44 GHz) for the lower band and 56% (4.59–8.16 GHz) for the upper band. The strong agreement between simulated and measured results validates the design's potential for practical and scalable implementation. This DBPA design offers a simpler, more compact, and wider-bandwidth alternative to conventional antennas, making it ideal for modern WLAN systems.

This is an open access article under the [CC BY-SA](#) license.



Corresponding Author:

Suthasinee Lamultree

Department of Electronics and Telecommunication Engineering, Faculty of Engineering

Rajamangala University of Technology Isan Khonkaen Campus

Khonkaen, 40000, Thailand

Email: suthasinee.la@rmuti.ac.th

1. INTRODUCTION

As mobile internet, internet of things (IoT), and Bluetooth technologies gain traction, routers and access point antennas have become essential components of wireless local area networks (WLANs), meeting the increasing demand for faster transmission speeds and enhanced security for mobile devices. Omnidirectional antennas are particularly well-suited for routers due to their extensive area coverage [1]–[3]. Wireless fidelity (Wi-Fi) has established itself as the standard for WLAN communications within the 2.4 and 5 GHz industrial, scientific, and medical (ISM) frequency bands, specifically from 2.4 to 2.485 GHz [3] and across several 5 GHz ranges: 5.150–5.350 GHz, 5.470–5.725 GHz, and 5.725–5.850 GHz [4]–[6]. The introduction of Wi-Fi 6E, which operates in the 6 GHz band (5.925–6.425 GHz) [7], [8], significantly broadens the available spectrum, alleviating congestion and interference, thereby providing faster and more stable connections, especially in densely populated areas. WLANs have proven beneficial for numerous countries, highlighting the antenna's role as a transceiver for electromagnetic waves an integral part of radio frequency front ends since antenna performance significantly impacts the overall efficacy of the

communication system. Dual-band antennas are preferred over single-band antennas for numerous advantages, making them ideal for homes and businesses seeking fast and reliable Wi-Fi. To improve mobility and convenience, antennas that operate across multiple frequency bands are increasingly sought after [9]–[16], enabling multifunctionality without requiring additional devices, such as multi-feeding networks [17], [18]. Dual-band antennas excel in providing coverage in the 2.4 and 5 GHz WLAN bands, with several innovative design techniques emerging recently that align with current standards.

Several compact, dual-band, omnidirectional antennas have been proposed in the literature. Early work, such as in [1], [5], [9], explored various techniques. For example, Guo *et al.* [1] utilized coupled feeds and parasitic elements for dual-band operation, but this approach suffered from low gain. Other approaches to achieving high gain included cavity and slot-dipole hybrids [2] and meander line monopoles [3], though these were single-band designs (2.4 GHz WLAN). A dual-band (2.4/5 GHz) WLAN loop-slot antenna using a common-mode current was presented in [5], offering improved gain. More recent designs have focused on increasing functionality and bandwidth. Acıkaya and Yıldırım [6] achieved dual-band operation for 2.4/5 GHz WLAN by combining asymmetrical cuts, matching circuitry, a filter, and a parasitic patch. A compact, though complex, defective ground structure (DGS) slotted double patch antenna for WLAN and 5G was proposed in [9]. The fractal geometry-based design introduces multiple resonant paths, enabling multi-resonant behavior across a wide frequency range; nonetheless, its geometry is complex [10]. Complex metamaterial-fractal-DGS structures [11] have been utilized for triple-band operation. Kaur *et al.* [12], a compact MIMO antenna is presented to support the GSM-900 and sub-6 GHz 5G bands; it is realized through the strategic use of an inverted T-shape ground plane, allowing for frequency agility without enlarging the antenna's footprint. Further advancements include a dual-band antenna using a series feeding technique and magnetic coupling to a parasitic patch for enhanced bandwidth [13]. A multi-resonant, electromagnetic-compatible, hybrid laser-direct-structuring antenna for 2.4/5/6 GHz WLAN, incorporating loop, parasitic strips, and stub tuning, was presented in [14]. Furthermore, a folded stepped-impedance aperture is employed to provide a dual-band filtering response, maintaining a compact size and low loss without the need for additional external filtering networks [15]. Characteristic mode theory was used in [16] to generate dual-band resonances. A dual-band antenna loaded with a duplexer-integrated balun was explored in [17]. Other approaches, like the metamaterial antennas in [19], continued to enhance dual-band operation for 2.4/5 GHz Wi-Fi. Multi-mode radiators were employed in [20] for multi-band operation, but this approach introduced complexity due to multi-excitation, coupling, and isolation requirements. Lamultree *et al.* [21], half-wavelength inverted U-slots were integrated into a radiating patch for dual-band omnidirectional operation. A partial ground plane and a parasitic element were used [22] to improve radiation properties and bandwidth. Finally, a complex 4×4 multiple input multiple output (MIMO) structure using half-mode and parasitic half-mode patches, achieving two distinct -6 dB bandwidths, was presented in [23]. Tri-band operation was completed in [24] using an asymmetric coplanar strip-fed antenna with multi-shaped radiating branches.

This work presents the design of a dual-band antenna tailored for 2.4/5 GHz WLAN and extended Wi-Fi 6E applications. The antenna features a simple, cost-effective, single-fed geometry with two transmission bands, covering frequencies from 2.4 to 2.485 GHz, 5.150 to 5.850 GHz, and 5.925 to 6.425 GHz. The key contributions of this work include: (i) a single antenna that supports two distinct transition bands for WLAN applications; (ii) an omnidirectional radiation pattern with improved gain for 2.4/5 GHz WLAN applications; (iii) parasitic elements are introduced that transform the antenna from a wideband to a dual-band design, enhancing its radiation performance; and (iv) the use of a single feed through a coplanar waveguide (CPW).

The structure of this paper is as: section 1 introduces the topic, and section 2 outlines the antenna design process, including the model, development of the dual-band patch antenna (DBPA), and initial formulas. Section 3 presents the antenna prototype along with numerical and measured results. Finally, section 4 concludes the work.

2. PROCEDURE SPECIFICALLY DESIGNED

2.1. Design layout

Figure 1 displays the layout of the dual-band patch antenna. The primary radiating component is a modified rectangular patch with dimensions width (w_r) and length (l_r), featuring a corner cut at an angle (α). Flanking the main patch are two parasitic rectangular patches, each measuring length l_p (33 mm) and width w_p (15 mm). All elements are constructed on a thick (t) copper layer, as depicted in Figure 1. The antenna is excited by a 50-Ohm coplanar waveguide with parameters width (w_g), length (l_g), and a 0.4 mm feed-to-ground gap (g). The complete structure is fabricated on a single-layer copper circuit board, with dimensions of $l \times w \times h$ (70×70×0.16 mm³), utilizing a flame-retardant 4 (FR4) base with a relative permittivity of 4.3 and a thickness (h) of 1.6 mm. The patch-to-ground plane separation, denoted as s_r , is 1.5 mm. In comparison, s_p (1 mm)

represents the spacing between the main radiating to parasitic patches. The parasitic patch height above the ground plane is h_p (21.5 mm). The design of the DBPA was carried out using computer simulation technology microwave studio [25]. Through iterative parameter modifications, the design was refined to ensure acceptable impedance characteristics ($|S_{11}| < -10$ dB) and effective omnidirectional radiation performance. The final optimized design parameters are summarized in Table 1.

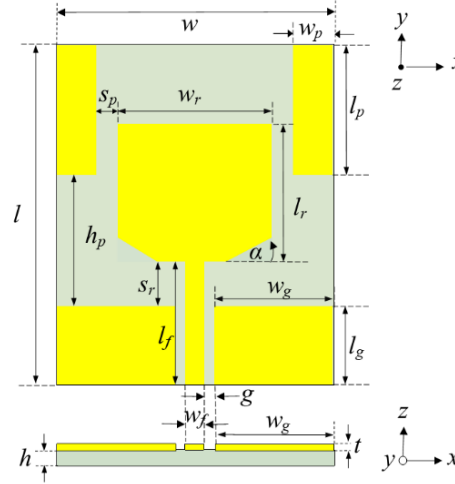


Figure 1. Layout of the DBPA

Table 1. Optimized parameter values for the DBPA

Variable	Parameter description	Dimension (mm)
w	Width of the base material	70
l	Length of the base material	70
l_r	Length of a rectangular patch	31
w_r	Width of a rectangular patch	38
l_p	Length of a rectangular parasitic	33
w_p	Width of a rectangular parasitic	15
α	Angle of the lower edge radiating patch-cutting	30°
h_p	Parasitic patch height above the ground plane	21.5
s_p	Radiating patch-parasitic separation	1
s_r	Separating patch-ground plane	1.5
l_f	Feeding-microstrip line length	17
w_f	Feeding-microstrip line width	3
l_g	Ground plane length	15.5
w_g	Ground plane width	33.1
g	Feed-to-ground gap	0.4
t	Copper layer thickness	0.035
h	Thickness of the base material	1.6

2.2. Stages of antenna design

The dual-band patch antenna was developed through a three-stage design process, as illustrated in Figure 2, where the first, second, and final designs are depicted in Figures 2(a) to (c), respectively. The first step, Antenna #1 (Figure 2(a)), involved creating a rectangular patch (38 mm × 31 mm) on a 1.6 mm thick FR4 base (70×70 mm). A 50-Ohm CPW feed, designed using (1)-(3) [26] for a 2.45 GHz resonance, was utilized. Figures 3, 4(a) to (c) summarize the $|S_{11}|$ and radiation patterns for each stage of this design evolution.

$$w_r = \frac{c}{2f_r} \sqrt{\frac{2}{\epsilon_r + 1}} \quad (1)$$

$$l_r = \frac{c}{2f_r \sqrt{\epsilon_{eff}}} - 0.824h \left[\frac{(\epsilon_{eff} + 0.3)(w_r + 0.264h)}{(\epsilon_{eff} - 0.258)(w_r + 0.8h)} \right] \quad (2)$$

where ϵ_{eff} is an effective dielectric constant.

$$\varepsilon_{\text{reff}} = \frac{\varepsilon_r + 1}{2} + \frac{\varepsilon_r - 1}{2} \sqrt{1 + \frac{12h}{w_r}} \quad (3)$$

Meanwhile, the width (w_f) and length (l_f) of 3 mm and 17 mm, respectively, are computed for a 50-Ω impedance using the following (4)-(5) [26].

$$w_f = \frac{2h}{\pi} \left\{ \left(\frac{60\pi^2}{Z_0 \sqrt{\varepsilon_r}} \right) - 1 - \ln \left(\frac{120\pi^2}{Z_0 \sqrt{\varepsilon_r}} - 1 \right) + \frac{\varepsilon_r - 1}{2\varepsilon_r} \left(\ln \left(\frac{60\pi^2}{Z_0 \sqrt{\varepsilon_r}} - 1 \right) + 0.39 - \frac{0.61}{\varepsilon_r} \right) \right\} \quad (4)$$

$$l_f = \frac{\lambda_g}{4} \quad (5)$$

where λ_g is the guide wavelength.

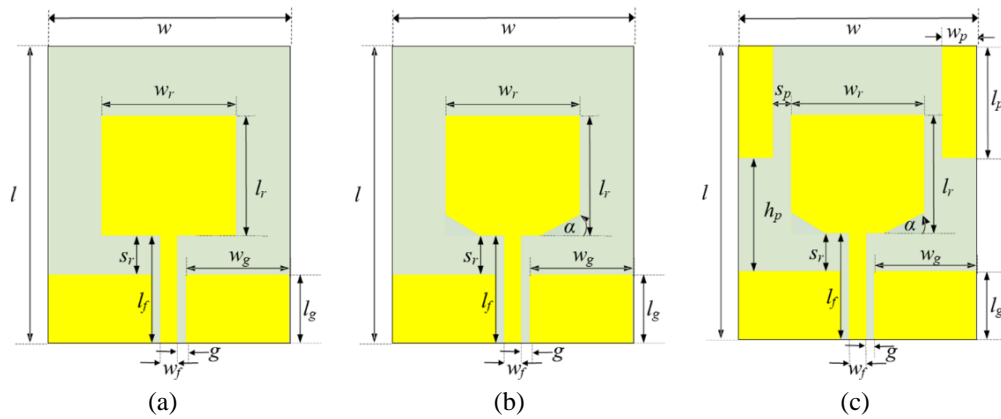


Figure 2. The developed antenna: (a) Ant#1, (b) Ant#2, and (c) proposed DBPA

To achieve 50-Ohm impedance matching, a 0.4 mm gap (g) was implemented between the feed line and ground plane, as calculated using methods from [27], [28] (see (6)-(10) in [28]). The ground plane extended 15.5 mm beyond the radiating rectangular patch (RRP) edge, and a 1.5 mm separation (s_r) was maintained between the RRP and the ground plane. Antenna #2 is derived from Antenna #1 by modifying the patch's bottom corner at an angle (α), as shown in Figure 2(b). In the last design phase, parasitic patches are introduced to enhance antenna performance. These patches, with widths (w_p) and lengths (l_p), are strategically positioned on either side of the main patch, elevated at a height (h_p) above the ground plane (as shown in Figure 2(c)). The dimensions of the parasitic patches are interrelated: as w_p increases, s_p decreases. Similarly, l_p and h_p have an inverse relationship; longer l_p requires a shorter h_p . The main radiator measures 38 mm in width (w_r) and 31 mm in length (l_r), with the parasitic patches extending 16 mm from the base edge towards the main radiator.

The design progression involved three distinct prototypes, each optimized to achieve specific performance goals. Antenna #1 served as the baseline design. It produced a stable omnidirectional radiation pattern with peak gains of 2.14 dBi at 2.45 GHz and 4.25 dBi at 5.5 GHz. This initial design demonstrated acceptable but limited bandwidths of 1.92–3.11 GHz and 4.78–5.66 GHz. The performance characteristics of Antenna #1 are visually represented in Figures 3 and 4(a). Antenna #2 introduced a significant modification that maintained the omnidirectional pattern while substantially improving the bandwidth. The peak gains shifted slightly to 2.08 dBi at 2.45 GHz and 4.95 dBi at 5.5 GHz. More importantly, the 10 dB return loss bandwidth expanded dramatically to 1.78–6.77 GHz and 7.96–8.47 GHz, as shown in Figures 3 and 4(b). This modification proved that a wideband response was achievable. The final antenna combines the best attributes of the previous prototypes. It successfully maintains an omnidirectional radiation pattern while achieving two broad bandwidths: 1.64–3.49 GHz and 4.38–6.75 GHz. This final iteration delivers competitive gains of 3.03 dBi at 2.45 GHz and 4.59 dBi at 5.5 GHz. The detailed results for this optimized design are presented in Figures 3 and 4(c). This progression from Antenna #1 to the final design demonstrates a methodical approach to optimizing both bandwidth and gain while preserving the essential omnidirectional pattern.

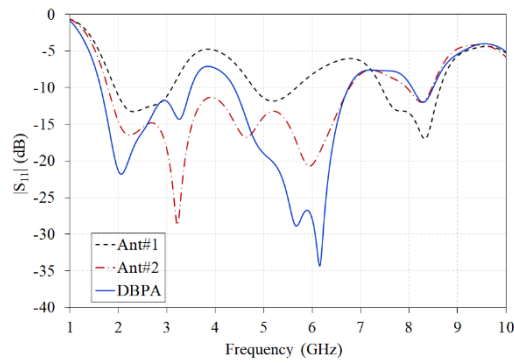


Figure 3. Comparing simulated $|S_{11}|$ of the developed antenna

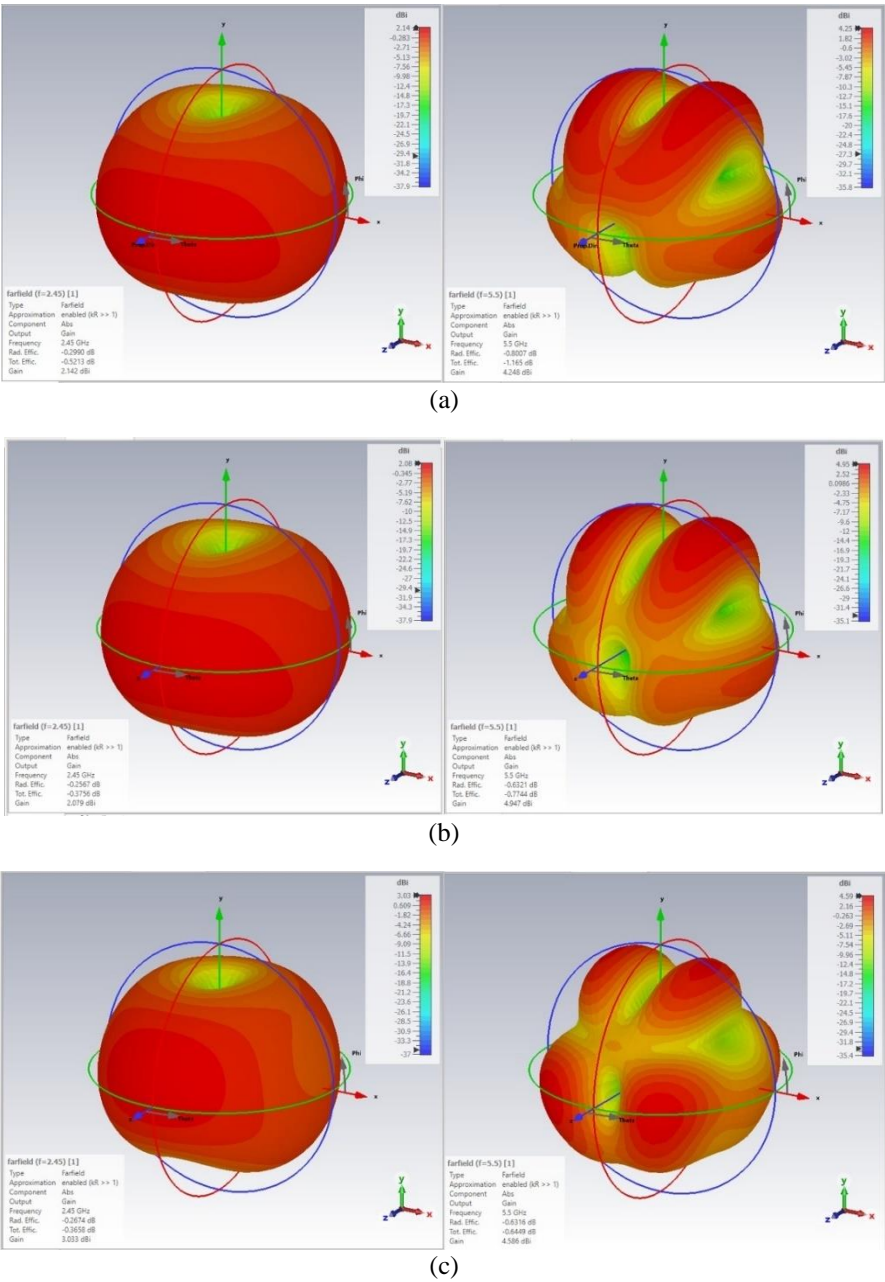


Figure 4. 3D radiation pattern of (a) Ant#1, (b) Ant#2, and (c) DBPA

A parametric study was conducted to evaluate the effect of the cutting angle (α) on the impedance bandwidth. Figure 5 illustrates the simulated reflection coefficient ($|S_{11}|$) for angles ranging from 0° to 90° . The results reveal a clear relationship: a smaller cutting angle leads to a wider -10 dB bandwidth. Based on this analysis, the α of 30° was chosen to achieve the broadest possible bandwidth. For context, the α of 0° corresponds to the original Antenna #1 geometry, and the α of 90° represents a modified, narrower rectangular shape.

The influence of w_p and l_p on $|S_{11}|$ was then evaluated in Figures 6 and 7. Various w_p values (6 mm to 16 mm) were tested, with corresponding changes in s_p (20 mm to 0 mm), while maintaining l_p at 33 mm and h_p at 21.5 mm. Figure 6 reveals that a narrower w_p resulted in degraded $|S_{11}|$ performance. A w_p of 16 mm achieved a wider dual-band response but shifted the lower-band operating frequency compared to $w_p=15$ mm. Therefore, $w_p=15$ mm and $s_p=1$ mm were selected to assess the effect of varying l_p values on $|S_{11}|$ as in Figure 7. Increasing l_p decreased $|S_{11}|$ at the lower band and shifted its resonance frequency downwards. Among the tested l_p values (27 mm to 39 mm), 33 mm was chosen for its effective 10 dB return loss across the 2.4/5 GHz WAN bandwidths and improved $|S_{11}|$ at the desired frequencies. This design achieved 10 dB return loss bandwidths of 1.64–3.49 GHz (lower band) and 4.38–6.75 GHz (upper band). It was observed that decreasing h_p reduced $|S_{11}|$ performance. In addition, gain and radiation efficiency were examined as shown in Figure 8. The final design exhibits an omnidirectional radiation pattern with gains ranging from 2.28 dBi to 4.49 dBi for the lower band, and 3.06 dBi to 5.01 dBi for the upper band. The corresponding radiation efficiencies ranged from 86.92% to 96.58% for the lower band, and 77.64% to 87.64% for the upper band.

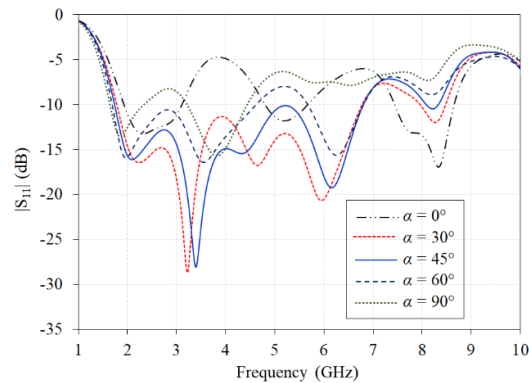
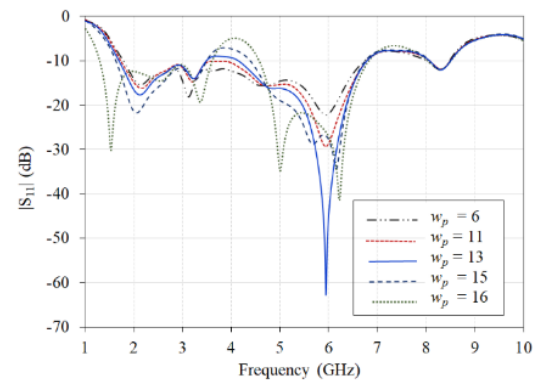
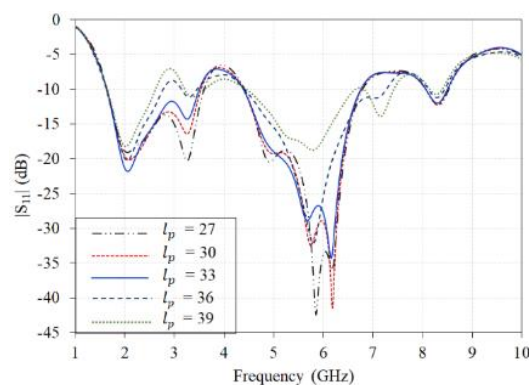
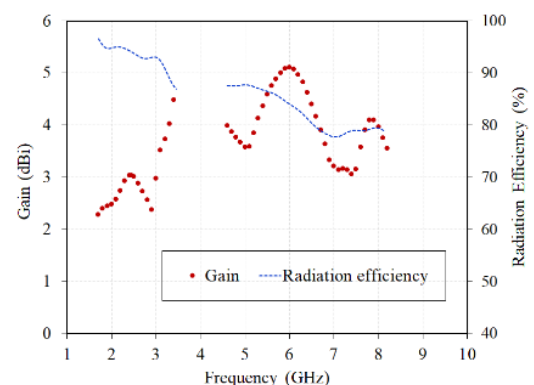
Figure 5. $|S_{11}|$ as the function of α Figure 6. $|S_{11}|$ as the function of w_p Figure 7. $|S_{11}|$ as the function of l_p 

Figure 8. Simulation results: gain and radiation efficiency

3. EXPERIMENTAL RESULTS AND THEIR IMPLICATIONS

To validate the numerical results, a prototype of the DBPA was fabricated on an FR4 base (relative permittivity of 4.3) according to the dimensions specified in Table 1. Figure 9(a) shows the top view of the fabricated prototype. The DBPA prototype was connected to a 50-ohm subminiature version A connector for coaxial feeding. Using an E5063A network analyzer (Figure 9(b)), $|S_{11}|$, 2D radiation patterns, and antenna

gain were measured. Figure 10 compares simulated and measured $|S_{11}|$ and gain. Both data sets exhibit a similar trend, with minimal discrepancies likely attributed to minor differences between the simulation and measurement setups, such as the solder joint at the 50-Ohm subminiature version A connector. The -10 dB bandwidths for WLAN applications were simulation: 1.64-3.49 GHz (72.2%), 4.38-6.75 GHz (42.6%), and measurement: 1.77-3.48 GHz (65.3%), 4.6-8.29 GHz (57.3%). In terms of radiation properties, the simulated peak gains of 3.03 dBi at 2.45 GHz and 4.58 dBi at 5.5 GHz were slightly higher than the measured gains of 2.92 dBi and 4.25 dBi, respectively.

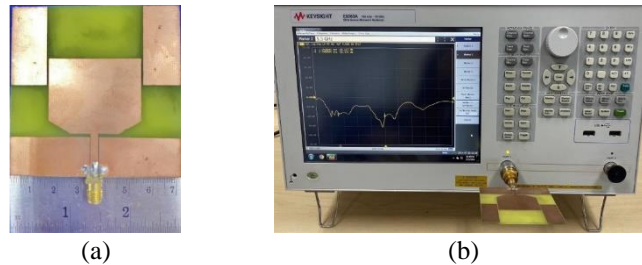


Figure 9. The DBPA prototype: (a) top view and (b) measurement

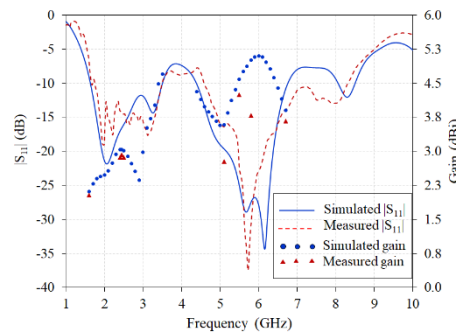


Figure 10. Validation of DBPA performance: simulated vs measured $|S_{11}|$ and gain

The radiation patterns of the dual-band patch antenna were measured at 2.45 GHz and 5.5 GHz in the xz - and yz -planes using identical antennas for transmission and reception. The measured patterns showed strong agreement with the simulated results. At 2.45 GHz, the antenna exhibits a nearly omnidirectional radiation pattern. The 3D pattern (Figure 11(a)) and the 2D xz -plane cut (Figure 11(b)) both confirm a consistent field strength in all directions. The yz -plane pattern shows a figure-eight shape (Figure 11(c)), which is characteristic of this omnidirectional behavior. At 5.5 GHz, the radiation pattern remains generally omnidirectional, although some splitting is observed (Figure 12(a)). The 2D representations in the xz - and yz -planes (Figures 12(b) and 12(c), respectively) show a broad omnidirectional pattern and a figure-eight shape, like the low-band behavior. Throughout the simulation process, the antenna maintains a linear polarization with a 40 dB axial ratio and low cross-polarization (below -30 dB) at both operating frequencies.

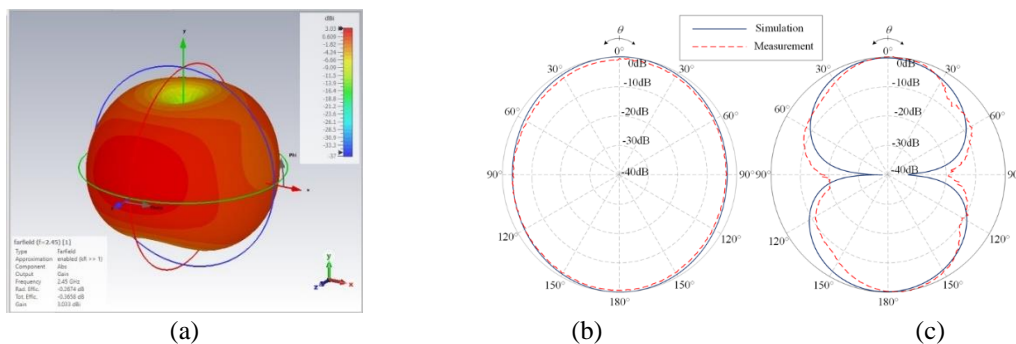


Figure 11. Simulated and measured radiation patterns at 2.45 GHz: (a) 3D, (b) xz -plane, and (c) yz -plane

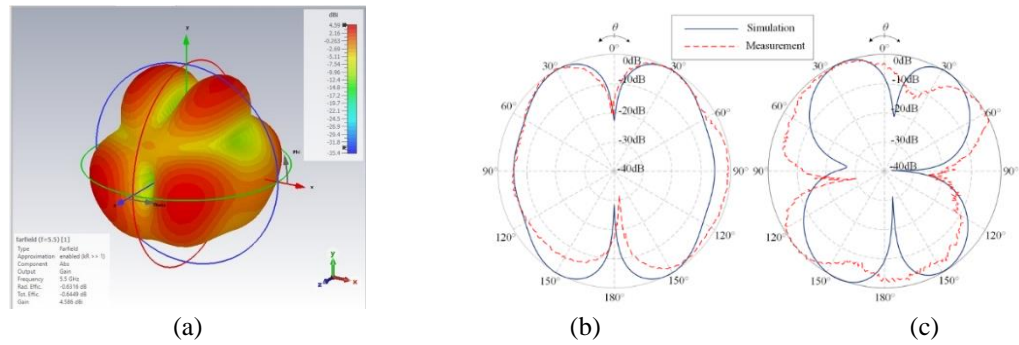


Figure 12. Simulated and measured radiation patterns at 5.5 GHz: (a) 3D, (b) xz -plane, and (c) yz -plane

A comparison of the proposed antenna with other designs for WLAN applications, based on their properties, is summarized in Table 2. The unbiased comparison uses the normalized antenna dimension $-\lambda_L$, representing the free-space wavelength at the lowest operating frequency. Key features for comparison include antenna type, material, dimension, bandwidth, pattern, structure complexity, gain, and efficiency. It's worth noting that most of the compared antennas provide linear polarization. The polarization of some designs was not specified in their respective papers. The proposed antenna is fabricated on an FR4 substrate, like several other designs [19]–[21]. It is also categorized as having a less complex structure, which is comparable to the antennas in [1], [19], [21], but simpler than designs such as the MIMO system in [20] or the DGS slotted double patch in [9]. The antenna achieves an omnidirectional radiation pattern, a characteristic shared with designs in [1], [2], [5], [9], [21], but unlike the directional or unidirectional patterns seen in other works [19], [20]. In terms of radiation efficiency, this work offers similar performance to those in [2], [20], [21], though it is lower than the efficiency reported in [3]. A key advantage of this design is its notably wide bandwidth, with a 10 dB return loss bandwidth of 67.7% (1.7–3.44 GHz) for the lower band and 56% (4.59–8.16 GHz) for the upper band. This is significantly wider than the bandwidths of the antennas in [1]–[3], [5], [21]. For instance, while the design in [21] covers the standard 2.4–2.8 GHz and 4.96–5.86 GHz ranges, the proposed antenna's extended bands are well-suited to support emerging Wi-Fi 6E requirements. This antenna also provides competitive gains of 2.92 dBi at 2.4 GHz and 4.25 dBi at 5 GHz. While the antenna in [2] achieves a higher gain, its structure is more complex (an 8-element array). The gains of this work are also higher than the gains reported in [1], [5], [21]. Overall, the proposed design offers a compelling trade-off between structural simplicity, compact size ($39.67 \text{ m}\lambda_L \times 39.67 \text{ m}\lambda_L \times 0.91 \text{ m}\lambda_L$), enhanced performance, and extended bandwidth for Wi-Fi 6E, making it well-suited for modern WLAN systems.

Table 2. Quality comparisons

Ref.	Antenna type	Material	Dimension ($\text{m}\lambda_L$)	Bandwidth	Pattern	Structure complexity	Gain (dBi)	Efficiency (%)
[1]	3-D slots	Metal box	17.45×7.93×11.9	2.38–2.51 GHz, 4.8–5.9 GHz	Omni	Less	1.6, 2.3	n/a
[2]	8-array of a cavity and slot-dipole hybrid structure	F4BM	L×0.6L(n/a)×99.58	2.39–2.49 GHz	Omni	More	10	<83
[3]	Printed meander line patch antenna	RT5880	71.78×11.85×1.24	2.37–2.46 GHz	Quasi-omni	Medium	2.8	97
[5]	3-sector loop-slot with stub and CMC	Metal	25.08×276.52×N/A	2.15–2.65 GHz, 4.85–5.92 GHz	Omni	Medium	0.95, 2.43	n/a
[9]	DGS slots double-patch	RT5880	40.5×40.5×0.42	2.45–2.495 GHz, 5.0–6.3 GHz, 23–28 GHz	Omni	More	n/a, 4.72, 5.85	n/a
[19]	Metamaterial	FR4	28.85×37.51×1.44	2.164–2.638 GHz, 4.48–5.812 GHz	Direct	Less	3.24, 3.5	n/a
[20]	MIMO	FR4	90×37.5×4.05	2.25–2.63 GHz, 5.14–6.06 GHz	Uni	More	5.2, 6.7	81, 70.7
[21]	Patch with slots	FR4	38×30×1.28	2.4–2.8 GHz, 4.96–5.86 GHz	Omni	Less	2.55, 3.3	<86.34, <69.65
This work	Patch with parasitic	FR4	39.67×39.67×0.91	1.7–3.44 GHz, 4.59–8.16 GHz	Omni	Less	2.92, 4.25	<86.92, <77.64

Abbreviations: uni (unidirectional), omni (omnidirectional), direct (directional), and n/a (not applicable)

4. CONCLUSION

This paper introduces a novel dual-band modified rectangular patch antenna that leverages parasitic rectangular elements to transform a wideband response into two distinct resonant bands, enabling efficient operation across the 2.4–2.8 GHz, 4.96–5.86 GHz, and 5.925–6.425 GHz Wi-Fi/Wi-Fi 6E bands. The antenna, fabricated on a single-layer FR4 substrate and fed via a 50-Ohm coplanar waveguide, achieves omnidirectional radiation, linear polarization, and peak gains of 2.92 dBi at 2.45 GHz and 4.25 dBi at 5.5 GHz. Notably, it achieves impressively high radiation efficiencies of 94.02% (2.45 GHz) and 86.45% (5.5 GHz). The core innovation lies in the strategic use of parasitic patches, which enables dual-band operation without resorting to multilayer or complex geometries. This design offers a favorable trade-off between structural simplicity, ease of fabrication, and performance; however, it remains sensitive to physical tolerances and variations in operating environments, which can impact resonance stability and impedance matching. Future work will explore antenna array configurations based on this single-element design to enhance gain, as well as integration into real-world devices for mobile and IoT applications. This contribution advances wireless communication by offering a compact, efficient, and scalable antenna solution tailored to the evolving demands of modern WLAN systems.

ACKNOWLEDGEMENTS

We extend our sincere gratitude to Asst. Prof. Dr. Adirek Jantakun for his expert guidance on graphical elements.

FUNDING INFORMATION

This research project is supported by Science Research and Innovation Fund Agreement No. FF68/KKC/037.

AUTHOR CONTRIBUTIONS STATEMENT

This journal uses the Contributor Roles Taxonomy (CRediT) to recognize individual author contributions, reduce authorship disputes, and facilitate collaboration.

Name of Author	C	M	So	Va	Fo	I	R	D	O	E	Vi	Su	P	Fu
Suthasinee Lamultree	✓	✓		✓	✓	✓	✓	✓	✓	✓	✓			✓
Sakolkorn Ungprasutr		✓				✓	✓		✓					
Charinsak Saetiaiw	✓		✓							✓			✓	
Chuwong Phongcharoenpanich			✓		✓					✓		✓		

C : Conceptualization

M : Methodology

So : Software

Va : Validation

Fo : Formal analysis

I : Investigation

R : Resources

D : Data Curation

O : Writing - Original Draft

E : Writing - Review & Editing

Vi : Visualization

Su : Supervision

P : Project administration

Fu : Funding acquisition

CONFLICT OF INTEREST STATEMENT

The authors declare no conflict of interest.

DATA AVAILABILITY

Data availability does not apply to this paper.




REFERENCES

- [1] J. Guo, H. Bai, A. Feng, Y. Liu, Y. Huang, and X. Zhang, "A Compact Dual-Band Slot Antenna with Horizontally Polarized Omnidirectional Radiation," *IEEE Antennas and Wireless Propagation Letters*, vol. 20, no. 7, pp. 1234–1238, Jul. 2021, doi: 10.1109/LAWP.2021.3076169.
- [2] Y. Zhang and Y. Li, "Scalable Omnidirectional Dual-Polarized Antenna Using Cavity and Slot-Dipole Hybrid Structure," *IEEE Transactions on Antennas and Propagation*, vol. 70, no. 6, pp. 4215–4223, Jun. 2022, doi: 10.1109/TAP.2021.3138552.
- [3] H. H. Ibrahim *et al.*, "Low Profile Monopole Meander Line Antenna for WLAN Applications," *Sensors*, vol. 22, no. 16, p. 6180, Aug. 2022, doi: 10.3390/s22166180.
- [4] D. Sánchez-Hernández, *Multiband integrated antennas for 4G terminals*. 2008.




- [5] W. Song, Z. Weng, Y. C. Jiao, L. Wang, and H. W. Yu, "Omnidirectional WLAN Antenna with Common-Mode Current Suppression," *IEEE Transactions on Antennas and Propagation*, vol. 69, no. 9, pp. 5980–5985, Sep. 2021, doi: 10.1109/TAP.2021.3076261.
- [6] F. C. Acikaya and B. S. Yildirim, "A Dual-Band Microstrip Patch Antenna for 2.45/5-GHz WLAN Applications," *AEU - International Journal of Electronics and Communications*, vol. 141, p. 153957, Nov. 2021, doi: 10.1016/j.aeu.2021.153957.
- [7] N. Nurhayati, F. Y. Zulkifli, E. Setijadi, B. E. Sukoco, M. N. M. Yasin, and A. M. De Oliveira, "Bandwidth, Gain Improvement, and Notched-Band Frequency of SWB Wave Coplanar Vivaldi Antenna Using CSRR," *IEEE Access*, vol. 12, pp. 16926–16938, 2024, doi: 10.1109/ACCESS.2024.3359168.
- [8] K. L. Wong, T. C. Wei, Y. S. Tseng, and W. Y. Li, "Compact 2×2 Dual-Polarized Patch Antenna Array Transmitting Eight Uncorrelated Waves for the WiFi-6E MIMO Access Point Featuring Eight Spatial Streams," *IEEE Access*, vol. 12, pp. 36793–36809, 2024, doi: 10.1109/ACCESS.2024.3374378.
- [9] Z. Khan, M. H. Memon, S. Ur Rahman, M. Sajjad, F. Lin, and L. Sun, "A Single-fed Multiband Antenna for WLAN and 5G Applications," *Sensors (Switzerland)*, vol. 20, no. 21, pp. 1–13, Nov. 2020, doi: 10.3390/s20216332.
- [10] I. H. Nejdi, Y. Rhazi, M. A. Lafkih, S. Bri, and L. Mohammed, "A Novel Multi-Resonant and Wideband Fractal Antenna for Telecommunication Applications," *International Journal of Electrical and Computer Engineering*, vol. 12, no. 4, pp. 3850–3858, Aug. 2022, doi: 10.11591/ijece.v12i4.pp3850-3858.
- [11] A. Annou, S. Berhab, and F. Chebbara, "Metamaterial-Fractal-Defected Ground Structure Concepts Combining for Highly Miniaturized Triple-Band Antenna Design," *Journal of Microwaves, Optoelectronics and Electromagnetic Applications*, vol. 19, no. 4, pp. 522–541, Dec. 2020, doi: 10.1590/2179-10742020V19I4894.
- [12] N. Kaur *et al.*, "Two-Port/Four-Port Self-Isolated MIMO Antenna with Dual Band for GSM-900/Sub-6 GHz 5G Applications for IoT and Biomedical Applications," *International Journal of Numerical Modelling: Electronic Networks, Devices and Fields*, vol. 38, no. 5, pp. 1–19, Sep. 2025, doi: 10.1002/jnm.70110.
- [13] L. Chang and H. Liu, "Low-Profile and Miniaturized Dual-Band Microstrip Patch Antenna for 5G Mobile Terminals," *IEEE Transactions on Antennas and Propagation*, vol. 70, no. 3, pp. 2328–2333, Mar. 2022, doi: 10.1109/TAP.2021.3118730.
- [14] P. H. Juan and S. W. Su, "EMC Hybrid Loop/Monopole LDS Antenna with Three-Sided Ground Walls for 2.4/5/6 GHz WLAN Operation," *IEEE Antennas and Wireless Propagation Letters*, vol. 22, no. 9, pp. 2200–2204, Sep. 2023, doi: 10.1109/LAWP.2023.3281457.
- [15] H. Xu and K. -D. Xu, "A Single-Fed Dual-Band Orthogonal Circularly Polarized Filtering Antenna for 5G-Enabled IoV Applications," in *IEEE Internet of Things Journal*, doi: 10.1109/IIOT.2025.3608034.
- [16] P. S. B. Ghouse *et al.*, "A Compact Dual-Band Millimeter Wave Antenna for Smartwatch and IoT Applications with Link Budget Estimation," *Sensors*, vol. 24, no. 1, p. 103, Dec. 2024, doi: 10.3390/s24010103.
- [17] J. Li, J. Li, J. Yin, C. Guo, H. Zhai, and Z. Zhao, "A Miniaturized Dual-Band Dual-Polarized Base Station Antenna Loaded with Duplex Baluns," *IEEE Antennas and Wireless Propagation Letters*, vol. 22, no. 7, pp. 1756–1760, Jul. 2023, doi: 10.1109/LAWP.2023.3262824.
- [18] X. F. Li, Y. L. Ban, Q. Sun, Y. X. Che, J. Hu, and Z. Nie, "A Compact Dual-Band Van Atta Array Based on the Single-Port Single-Band/Dual-Band Antennas," *IEEE Antennas and Wireless Propagation Letters*, vol. 22, no. 4, pp. 888–892, Apr. 2023, doi: 10.1109/LAWP.2022.3227577.
- [19] X. Wu, X. Wen, J. Yang, S. Yang, and J. Xu, "Metamaterial Structure Based Dual-Band Antenna for WLAN," *IEEE Photonics Journal*, vol. 14, no. 2, pp. 1–5, Apr. 2022, doi: 10.1109/JPHOT.2022.3163170.
- [20] W. Zhang, Y. Li, K. Wei, and Z. Zhang, "A Dual-Band MIMO Antenna System for 2.4/5 GHz WLAN Applications," *IEEE Transactions on Antennas and Propagation*, vol. 71, no. 7, pp. 5749–5758, Jul. 2023, doi: 10.1109/TAP.2023.3277208.
- [21] S. Lamultree, N. Somsanook, W. Narkkoht, and C. Phongcharoenpanich, "A Dual-Band Rectangular Shape Incorporated Into Circular Patch Antenna for 2.4/5 Ghz Wireless Local Area Network Applications," *Telkomnika (Telecommunication Computing Electronics and Control)*, vol. 23, no. 1, pp. 22–31, Jan. 2025, doi: 10.12928/TELKOMNIKA.v23i1.26519.
- [22] L. C. Paul, H. K. Saha, T. Rani, M. Z. Mahmud, T. K. Roy, and W. S. Lee, "An Omni-Directional Wideband Patch Antenna with Parasitic Elements for Sub-6 GHz Band Applications," *International Journal of Antennas and Propagation*, vol. 2022, pp. 1–11, Oct. 2022, doi: 10.1155/2022/9645280.
- [23] X. Chen, J. Wang, and L. Chang, "Extremely Low-Profile Dual-Band Microstrip Patch Antenna Using Electric Coupling for 5G Mobile Terminal Applications," *IEEE Transactions on Antennas and Propagation*, vol. 71, no. 2, pp. 1895–1900, Feb. 2023, doi: 10.1109/TAP.2022.3217640.
- [24] Y. Rahayu, D. R. A. Pangestu, and C. H. Ku, "Compact Triple-Band Monopole Antenna with ACS-Fed for IoT Devices on WLAN/WiMAX/5G/V2X Networks," *International Journal of Electrical and Electronic Engineering and Telecommunications*, vol. 14, no. 1, pp. 43–50, 2025, doi: 10.18178/ijeetc.14.1.43-50.
- [25] "Microwave Studio." Computer Simulation Technology, 2016. [Online]. Available: <https://sigmasolutions.co.th/en/cst-studio-suite>
- [26] C. A. Balanis, *Antenna Theory: Analysis and Design*, 4th ed. Wiley, 2016.
- [27] R. E. Collin, *Foundations for Microwave Engineering*. New York: McGraw-Hill, 2010, doi: 10.1109/9780470544662.
- [28] S. Lamultree, S. Srisukhot, C. Saetia, K. Nuangwongsa, and C. Phongcharoenpanich, "Design of a Compact Wideband Bi-Directional Pattern Antenna for 5G Applications," *EUREKA, Physics and Engineering*, vol. 2023, no. 4, pp. 40–51, Jul. 2023, doi: 10.21303/2461-4262.2023.002855.

BIOGRAPHIES OF AUTHORS






Suthasinee Lamultree    received the B. Eng., and M. Eng., in Telecommunication Engineering from King Mongkut's Institute of Technology Ladkrabang, Thailand, in 2000 and 2003, respectively. In 2009, she received her D. Eng. in Electrical Engineering from the same institute. In 2016, she joined the Department of Electronics and Telecommunication Engineering, Faculty of Engineering, Rajamangala University of Technology Isan Khonkaen Campus, Khonkaen, Thailand. Her research interests include antenna design, microwave technology, and wireless communication systems. She can be contacted at email: suthasinee.la@rmuti.ac.th.






Sakolkorn Ungprasutr    received the B.Eng. in Electronics and Telecommunication Engineering from the Faculty of Engineering, Rajamangala University of Technology Isan Khonkaen Campus, Thailand, in 2023. His research interests include antenna and circuit design. He can be contacted at email: sakolkorn.un@rmuti.ac.th, sakolkorn.un@gmail.com.



Charinsak Saetiaw    received his Ph.D. in Telecommunication Engineering from Suranaree University of Technology in 2016. He is an Assistant Professor in the Department of Electronics and Telecommunication Engineering, Faculty of Engineering, at Rajamangala University of Technology Isan, Khon Kaen Campus. His research focuses on antenna design, wireless communication, telecommunication engineering, emerging technologies, and innovative applications. His work interests are the development of antennas for 4G and 5G applications, 3D printing and conductive materials, and advancing applications in wearable and vehicular communication systems. He can be contacted at email: charinsak.sa@rmuti.ac.th.



Chuwong Phongcharoenpanich    received his B.Eng. (Hons.), M.Eng., and D.Eng. degrees from King Mongkut's Institute of Technology Ladkrabang (KMITL), Bangkok, Thailand, in 1996, 1998, and 2001, respectively. Currently, he is the Professor of Telecommunication Engineering at the Department of Telecommunications Engineering, KMITL. He also serves as the head of the Innovative Antenna and Electromagnetic Applications Research Laboratory. His research interests are antenna design for various mobile and wireless communication devices, conformal antenna, and array antenna theory. He can be contacted at email: pchuwong@gmail.com.